Journal of Materials Chemistry C

Accepted Manuscript

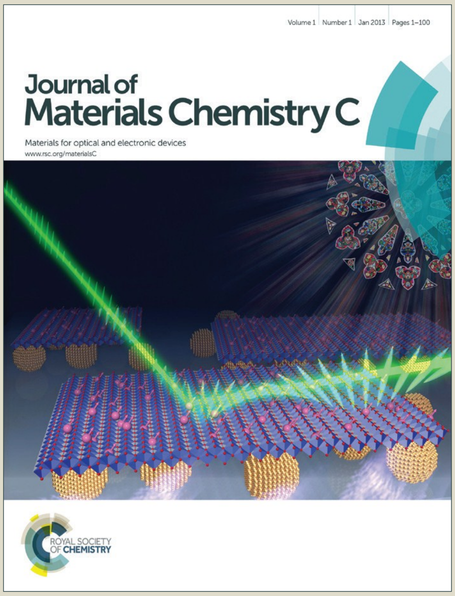

ROYAL SOCIETY OF CHEMISTRY

www.rsc.org/materialsC

Journal Name

COMMUNICATION

Near Room Temperature Plasma Enhanced Atomic Layer Deposition of Ruthenium using the RuO_4-precursor and H_2-plasma

Received 00th January 20xx,
Accepted 00th January 20xx

DOI: 10.1039/x0xx00000x

www.rsc.org/

Matthias M. Minjauw,[a] Jolien Dendooven,[a] Boris Capon,[a] Marc Schaekers[b] and Christophe Detavernier[a]

A plasma enhanced ALD process for Ru using RuO_4 and H_2-plasma is reported at sample temperatures ranging from 50°C to 100°C. At 50°C, low impurity content Ru thin films were grown with a saturated growth rate of 0.11 nm/cycle. A study of the influence of various process parameters on the Ru film properties is given.

The self-limited surface chemistry of atomic layer deposition (ALD) results in atomic level control over film thickness and ensures excellent uniformity and conformality on complex 3D substrates, rendering the technique uniquely suited for functionalization of nanostructures and nanomaterials.[1-3] In micro-electronics, metal ALD is therefore becoming increasingly important in view of the ever increasing aspect ratio of the nanostructured surface in novel device architectures.[4] One of the most attractive noble metals for applications in micro-electronics is Ru, because of its high work function (>4.7 eV), low bulk resistivity (7.1 µΩ.cm), high chemical and thermal stability and conductive oxide.[5,6] For these reasons, Ru ALD has been actively pursued during the past decade.

Both thermal[4] and plasma enhanced[7] Ru ALD processes have been reported in literature. For the thermal processes a metal-organic (MO) precursor, such as $RuCp_2$,[8] $Ru(EtCp)_2$,[9] $Ru(thd)_3$[10] or $Ru(DMPD)_2$,[11] is typically used in conjunction with molecular oxygen in a combustion chemistry. For the plasma enhanced processes, MO precursors have been used in combination with O_2-plasma (O_2*), NH_3-plasma (NH_3*) or a combined N_2+H_2-plasma ((N_2+H_2)*) as the reactant. Examples are the $RuCp(CO)_2/O_2$*,[12] $Ru(EtCp)_2/NH_3$*[13-15] and $Ru(MeCpPy)/(N_2+H_2)$*[16] processes. Benefits of using plasma are the capability to deposit at a lower substrate temperature, improved film purity and enhanced nucleation. Despite this, the share of reported plasma enhanced processes is still small.

Recently,[17] we reported a novel thermal Ru ALD process, using the inorganic RuO_4 precursor (ToRuS™, Air Liquide)[18] in combination with molecular hydrogen. It was proposed that during the first half-reaction RuO_2 is being deposited by a self saturated reaction of RuO_4 with the Ru-surface, and during the second half-reaction this deposited oxide is thermally reduced to Ru by H_2. The self-saturating behaviour of the first half-reaction can be explained as follows: once the unreacted metal is fully covered by RuO_2, the reaction stops as the RuO_2 surface is not able to react with or catalytically decompose RuO_4.[17] The first half-reaction presents an upper limit for the ALD process, as thermal decomposition of RuO_4 to RuO_2 was found to occur for sample temperatures just above 100°C, converting the ALD-process into a pulsed-CVD[19,20] (p-CVD) process. The second half-reaction on the other hand, presents a lower limit to the process, as thermal reduction of RuO_2 to Ru using H_2 requires at least 100°C.[17,21] Hence the thermal ALD process has a very narrow temperature window near 100°C.

In this communication, it is shown that the second half-reaction can be activated for temperatures below 100°C by replacing the molecular H_2-pulse by H_2-plasma (H_2*), while the first half-reaction remains active. The ALD-characteristics of the RuO_4/H_2*-process are derived and the purity, resistivity and crystallinity of the grown Ru thin films are determined. This is the first Ru PEALD process having a temperature window below 100°C, making it the lowest temperature Ru (PE)ALD-process reported so far.

The depositions were performed in an experimental ALD reactor with a base pressure of 10^{-6} mbar and a remote plasma configuration.[22] RuO_4 is a volatile toxic and explosive compound, and is a strong oxidizing agent such that it can react violently with various organic compounds. Therefore, the RuO_4 precursor was delivered to the reactor in the dissolved state (ToRuS™: diluted solution of RuO_4 in an inert organic solvent), as this reduces the potential hazards.[18] Furthermore, the solution was supplied by Air Liquide in a ready-to-use canister, which was connected to a pneumatically controlled inlet of the reactor through stainless steel tubing. The pressure of the precursor-pulse (ToRuS) was 4.5 10^{-3} mbar, while that of the plasma (20/80 H_2/Ar-mixture) was 5 10^{-3} mbar. Unless stated otherwise, the RuO_4-pulse lasted 60s and the H_2* pulse lasted 20s with a plasma power of 425W and a sample temperature of 50°C. The ALD-reactor is equipped with a Woollam M-2000 spectroscopic ellipsometer, enabling in situ spectroscopic ellipsometry (ISE). The crystallinity and thickness of the deposited films were determined by X-ray Diffraction (XRD) and X-ray Reflectivity (XRR) respectively, using a Bruker D8 diffractometer with a CuKα source. Electrical resistivity was determined using a 4-point probe. Surface roughness and morphology of the films was determined by Atomic Force Microscopy

---

[a] Department of Solid State Sciences, CoCooN, Ghent University, Krijgslaan 281 - S1, B-9000 Ghent, Belgium.
[b] IMEC, Kapeldreef 75, B-3001 Leuven, Belgium

(AFM) using a Bruker Dimension Edge system and Scanning Electron Microscopy (SEM) using a FEI Quanta 200F instrument respectively. The purity and chemical composition of the thin films was investigated by X-ray Photoelectron Spectroscopy (XPS) using a Theta Probe (Thermo Scientific) instrument.

Experiments to determine the ALD growth characteristics were performed on sputtered Pt (7 nm), as it was found that this results in steady state Ru ALD from the very first cycle, without any major nucleation delay. The growth per cycle (GPC) was determined by dividing the deposited Ru film thickness on Pt, as determined by XRR, by the number of cycles of the deposition. Experiments to study thin film properties were performed on H-terminated Si substrates (Si-H), typically by putting them along with the Pt-substrates on the same sample holder. These Si-H substrates were obtained by performing an HF-dip on a piece of B-doped p-type Si (4-6 Ω.cm) right before transfer to the ALD-reactor.

The saturation behaviour of both ALD half-cycles was verified on sputtered Pt substrates at a deposition temperature of 50°C. For the precursor pulse time, it was found that 50s are needed to reach full saturation, while for the reactant plasma, saturation could be achieved from a pulse time of 15s (Figure 1, a). The film deposited on Pt with an under-saturated H_2* pulse time of 10s was found to have a density of only about 60% of the bulk Ru value (according to XRR). This lower density can be attributed to O-impurities incorporated in the film at under-saturated plasma exposure.

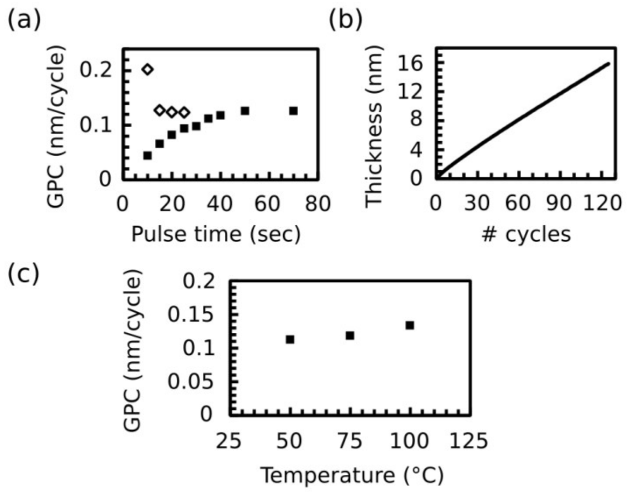

Figure 1. ALD characteristics of the RuO_4/H_2*-process. (a) GPC at 50°C as a function of the RuO_4 pulse time at a fixed H_2* pulse time of 15s (black squares), and as a function of the H_2* pulse time at a fixed RuO_4 pulse time of 60s (white diamonds). (b) Grown film thickness as a function of the number of cycles (c) Growth rate as a function of substrate temperature.

The influence of the H_2* pulse time on thin film properties was investigated by characterising Ru films deposited on Si-H substrates at 50°C (Table 1). No clear trend can be seen for the RMS roughness of the films as a function of H_2* pulse time, but the resistivity was found to decrease with increasing pulse times. XPS indicated the presence of oxygen next to Ru in the bulk of the films, while all other impurities were below the detection limit. The amount of oxygen was found to decrease with increasing H_2* pulse time, which can be understood by a more complete removal of oxygen by longer H_2* exposure.

The linearity of the process was verified by performing the saturated process over 125 cycles on sputtered Pt at 50°C, and monitoring it with ISE (Figure 1, b). The process is linear virtually from the start, with a steady state growth rate of about 0.11 nm/cycle.

Table 1. Thickness *Δ*, RMS roughness *R*, relative atomic concentration of oxygen (“*O*”) to ruthenium, and resistivity *ρ* of the Ru films deposited onto Si-H at 50°C and using different H_2 plasma pulse times t_p.

t_p (s)	# Cycles	*Δ* (nm)	*R* (nm)	*O* (at.%)	*ρ* (µΩ.cm)
10	125	14.9	0.3	7	53
15	125	16.4	0.2	5	29
20	125	16.1	0.3	4	27
25	125	14.7	0.4	3	27

The temperature window was determined by carrying out the process over 125 cycles on sputtered Pt substrates at sample temperatures of 50°C, 75°C and 100°C (Figure 1, c). Temperatures higher than 100°C were not considered because our previous work showed that thermal decomposition of RuO_4 starts to occur there. Temperatures lower than 50°C were not possible due to the fact that the chamber walls are put at 45°C to avoid condensation of the precursor. As can be seen on the figure, the growth rate increases slightly with temperature.

The influence of substrate temperature on thin film properties was determined (Table 2). The RMS roughness and thin film resistivity were both found to decrease with increasing temperature. XPS indicated oxygen as the only impurity in the bulk of the films, and the oxygen content slightly decreases with increasing temperatures.

Table 2. Thickness *Δ*, RMS roughness *R*, relative atomic concentration of oxygen (“*O*”) to ruthenium, and resistivity *ρ* of the Ru films deposited onto Si-H at different temperatures *T* and using a plasma pulse time of 20s.

T	# Cycles	*Δ* (nm)	*R* (nm)	*O* (at.%)	*ρ* (µΩ.cm)
50°C	125	16.1	0.3	4	27
75°C	125	16.7	0.2	2	24
100°C	125	17.8	0.1	<2	19

The influence of the H_2 plasma power on the physical properties of the Ru film was investigated at 50°C. Here, no clear trends were observed, and the roughness, purity and resistivity of the Ru films were found to be similar for H_2* powers of 150W, 250W, 350W and 425W.

For all explored process conditions, the Ru films were found to be polycrystalline hcp Ru, and the diffractogram for a film grown with the standard process is shown in Figure 2.

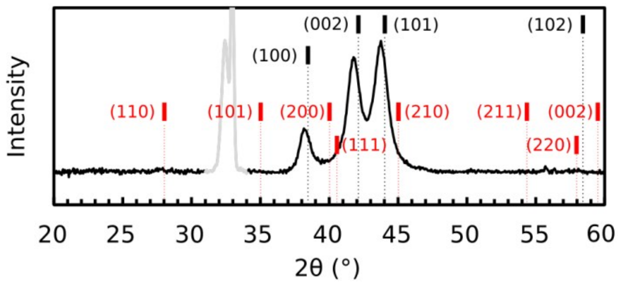

Figure 2. XRD diffractogram for the 16.1 nm Ru film grown at 50°C with a 60s RuO_4-pulse and a 20s H_2*-pulse of 425W. The two grey peaks are Si (002) peaks of the substrate and XRD sample cup. The expected peak positions for hcp Ru and rutile RuO_2 are indicated by the black and red vertical bars respectively.

The main conclusion of this work is that the second half-reaction, which was inactive for temperatures below 100°C in the thermal process using molecular H_2,[17] can be reactivated at these temperatures by replacing it with H_2 plasma. As such, we obtain the lowest temperature (PE)ALD-process reported so far. Together with our previous work (thermal ALD)[17] and earlier work by Han et al (pulsed-CVD),[19,20] this has allowed us to develop a better and more complete understanding of the RuO_4/H_2-process and its reaction mechanisms (Figure 3).

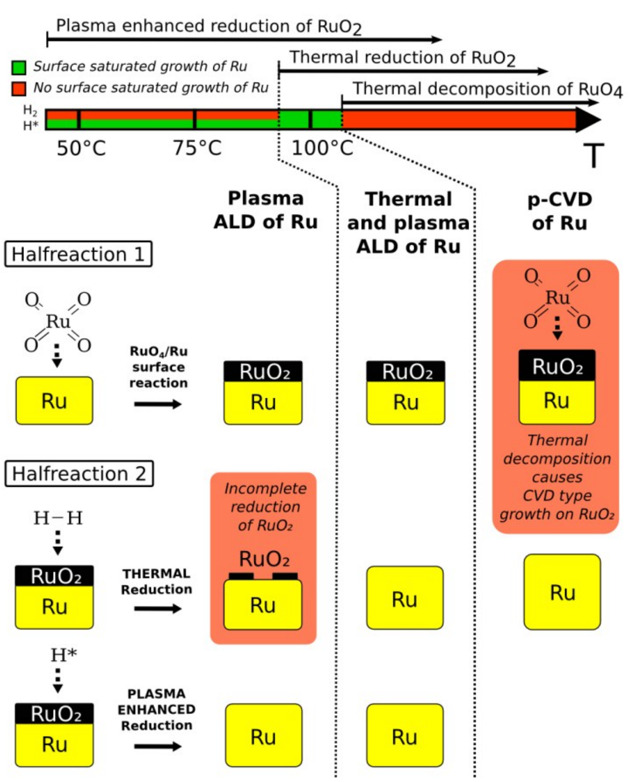

Figure 3. Schematic, summarizing the findings for the thermal and the plasma enhanced processes along the temperature axis.

As an illustration of the low temperature nature of the RuO_4/H_2*-process, deposition on polymers was attempted. For this, pieces of polypropylene (PP), low density polyethylene (PE-LD) and polystyrene (PS) were put into the reactor at a temperature of 50°C. The saturated RuO_4/H_2*-process was performed over 125 cycles, with a H_2 plasma power of 250W, and a picture of the samples after deposition is shown in Figure 4. It is clear that a Ru thin film was deposited on every polymer, and the polymers didn't degrade during the experiment. All three films survived a scotch tape test, which implies that film adhesion to the polymer is good. As RuO_4 is a strong oxidizing agent and is known to oxidize virtually any hydrocarbon, we expect that such an oxidation reaction of the polymer surface by RuO_4 leads to the first deposition of Ru atoms on the polymer, and can possibly explain the good adhesion of the Ru films to the polymers.

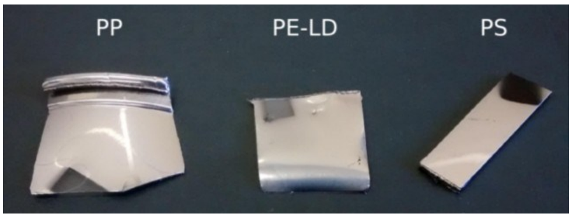

Figure 4. Picture of the Ru films grown on different types of polymers.

Acknowledgements

This research was supported by the Flemish Research Foundation FWO and BOF-UGent (GOA no. 01G01513). Matthias Minjauw and Jolien Dendooven acknowledge funding by FWO Vlaanderen.

Notes and references

1 R. L. Puurunen, *J. Appl. Phys.*, 2005, **97**, 121301.
2 S. M. George, *Chem. Rev.*, 2010, **110**, 111.
3 V. Miikkulainen, M. Leskelä, M. Ritala and R. L. Puurunen, *J. Appl. Phys.*, 2013, **113**, 021301.
4 J. Hämäläinen, M. Ritala and M. Leskelä, *Chem. Mater.*, 2014, **26**, 786.
5 International Technology Roadmap for Semiconductors 2011 and 2013. www.itrs.net (accessed Jan 28, 2015).
6 Tables of Physical & Chemical Constants, 16th edition 1995. Kaye & Laby Online. Version 1.0 (2005) www.kayelaby.npl.co.uk (accessed Mar 3, 2015).
7 H. B. Profijt, S. E. Potts and M. C. M. van de Sanden, W. M. M. J. Kessels, *J. Vac. Sci. Technol. A,* 2011, **29**, 050801.
8 T. Aaltonen, P. Alén, M. Ritala and M. Leskelä, *Chem. Vap. Depos.*, 2003, **9**, 45.
9 O.-K. Kwon, J.-H. Kim, H.-S. Park and S.-W. Kang, *J. Electrochem. Soc.*, 2004, **151**, 109.
10 T. Aaltonen, M. Ritala, K. Arstila, J. Keinonen and M. Leskelä, *Chem. Vap. Depos.*, 2004, **10**, 215.
11 R. Methaapanon, S. M. Geyer, H.-B.-R. Lee and S. F. Bent, *J. Mater. Chem.*, 2012, **22**, 25154.
12 N. Leick, S. Agarwal, A, J. M. Mackus and W. M. M. Kessels, *Chem. Mater.*, 2012, **24**, 3696.
13 O.-K. Kwon, S.-H. Kwon, H.-S. Park and S.-W. Kang, *J. Electrochem. Soc.*, 2004, **151**, C753.
14 Q. Xie, Y. L. Jiang, J. Musschoot, D. Deduytsche, C. Detavernier, R. L. Van Meirhaeghe, S. Van den Berghe, G. P. Ru, B. Z. Li and X. P. Qu, *Thin Solid Films*, 2009, **517**, 4689.
15 J. Musschoot, Q. Xie, D. Deduytsche, K. De Keyser, D. Longrie, J. Haemers, S. Van Den Berghe, R. L. Van Meirhaeghe, J. D' Haen and C. Detavernier, *Microelectron. Eng.*, 2010, **87**, 1879.
16 J. Swerts, A. Delabie, M. M. Salimullah, M. Popovici, M.-S. Kim, M. Schaekers and S. Van Elshocht, *ECS Solid State Lett*, 2012, **1**, P19.
17 M. M. Minjauw, J. Dendooven, B. Capon, M. Schaekers and C. Detavernier, *J. Mater. Chem. C*, 2015, **3**, 132.
18 J. Gatineau, K. Yanagita, C. Dussarrat, *Microelectron. Eng.*, 2006, **83**, 2248.
19 J. H. Han, S. W. Lee, G.-J. Choi, S. Y. Lee, C. S. Hwang, C. Dussarrat and J. Gatineau, *Chem. Mater.*, 2009, **21**, 207.
20 J. H. Han, S. W. Lee, S. K. Kim, S. Han, C. S. Hwang, C. Dussarrat and J. Gatineau, *Chem. Mater.*, 2010, **22**, 5700.
21 D. Ugur, A. J. Storm, R. Verberk, J. C. Brouwer and W. G. Sloof, *J. Phys. Chem. C*, 2012, **116**, 26822.
22 J. Musschoot, Q. Xie, D. Deduytsche, S. Van den Berghe, R. L. Van Meirhaeghe and C. Detavernier, *Microelectron. Eng.*, 2009, **86**, 72.

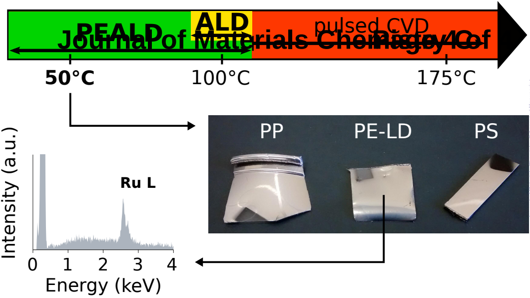
PEALD
ALD
pulsed CVD
50°C
100°C
175°C
PP
PE-LD
PS
Intensity (a.u.)
Ru L
0
1
2
3
4
Energy (keV)